JuniKhyat
ISSN: 2278-4632

(UGC Care Group I Listed Journal)
Vol-10 Issue-02 Nov 2020

Grading Glaucoma Stages using Wavelet Transform

Salil Kumar Malla,
College of Engineering Bhubaneswar

***Abstract*—A persistent eye condition called glaucoma damages the optic nerve and can result in irreversible vision loss. The traditional instrument approaches for glaucoma detection are laborious and tedious. Recently, a number of methods for automatically classifying glaucoma using retinal fundus pictures have been proposed.Nevertheless, none of the current techniques is effective for early-stage glaucoma identification.We presented a novel approach to classifying glaucoma in this letter, based on the recently developed two-dimensional tensor empirical wavelet transform (2D-T-EWT). In this study, 2D-T-EWT is used to breakdown the pre-processed images into sub-band images (SBIs). Next, from the decomposed SBIs, texture-based grey level-occurrence matrix (GLCM), chiphistogram, and moment invariant features were recovered. Robust features have already been chosen and ranked according to the student test algorithm.Ultimately, a trained multi-class support vector machine (MC-LS-SVM) classifier has been employed for the classification process.The experimental results demonstrate that our strategy for classifying glaucoma performed better than state-of-the-art approaches. Tenfold cross-validation was used in the suggested approach to attain the best classification accuracy of 93.65%.**

***Index Terms*—Glaucoma, fundus images, empirical wavelet transform, feature extraction, multiclass classification.**

I. INTRODUCTION

GLAUCOMA is a chronicretinal disease caused due to increasedintraocularpressure (IOP)intheopticnerve[1].I tharmstheopticnerve and eventuallycausesirreversiblevision loss[2].The effect of glaucoma is gradual increases that cannot be detected earlier until the condition is atanadvanced stage[3]. Theworldhealthorganization(WHO)providestheinternational classification of diseases (ICD) codes. In ICD tenth revision-clinicalmodification(ICD-10-CM)codes,365.71,365.72,and 365.73 are given for the early-stage (mild stage), moderate-stage, and advanced-stage (severe stage), respectively [3], [4]. The vision loss effects with various stages of glaucoma are shown in Fig. 1.

Many diagnostic tools used in the medical departments are asfollows.Tonometryismostlyusedasadiagnostictoolto

Fig.1.Visonlosseffectsatvariousstagesofglaucoma,(a)Normal(b)Early-stage glaucoma (c) Advanced-stage glaucoma.

measure IOP [5]. Perimetry is used to determine visual field loss, and stereo disc photography is helping to determine if there is unhealthy cupping in the optic nerve head (ONH) [3], [5].Thesemethods arelaborious,sluggish,requiredproficient clinician. Hence, computer-based methods are needed for the early, reliable and accurate diagnosis of glaucoma.

Recently,manyapproachesareproposedforautomaticglau-coma detection using retinal fundus. In related studies, Kirar*et al.* [6] used the concatenation of discrete wavelet transform (DWT) and empirical wavelet transform (EWT). Maheshwari *et al.* [7] and [8] Proposed EWT and variational mode decom-position(VMD)basedmethods,respectively.Agrawal*etal.* [9] investigated the image decomposition-based algorithm for glaucoma prediction using quasi-bivariate VMD (QB-VMD). Acharya *et al.* [10] extracted higher order spectra (HOS) and texture features from retinal images. In the different study [11], they use bi-dimensional empirical mode decomposition (BD-EMD) for extraction of entropy and energy features for glaucoma detection. Recently, Li *et al.* [12] presented a deep learning approach for glaucoma detection using a convolutional neural network (CNN) model. These methods have recently been usedforthediagnosisofglaucoma.However,theclassification of glaucoma stages is very crucial for the early and reliable diagnosis of glaucoma. For glaucoma classification, Noronha *et al.* [13] proposed the automatic method based on radon transform (RT) they use 272 fundus images from the private databaseandclassifiedintohealthy,mild,andsevereglaucoma. Thefundusimagesofvariousstagesofglaucomaareshownin Fig. 2.

Intheliterature,theconventionalmethods[2],[11]havebeen used for glaucoma detection. In which DWT based algorithm [2] are non-adaptive and limited to dyadic scale. The draw-backsofthedyadicDWTbasedapproachareasfollows:Shift-invariance, constant time-frequency covering, low-frequency resolution,andsignalindependently.However,theconventional EMD-based method [11] having limitations such as bound-ary distortion, lack of mathematical theory, and mode mixing problem. Besides, EMD based decomposition highly depends

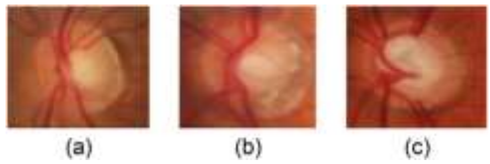

Fig. 2.Fundus images, (a) Normal image (b) Early-stage glaucoma (c)Advanced-stageglaucoma.

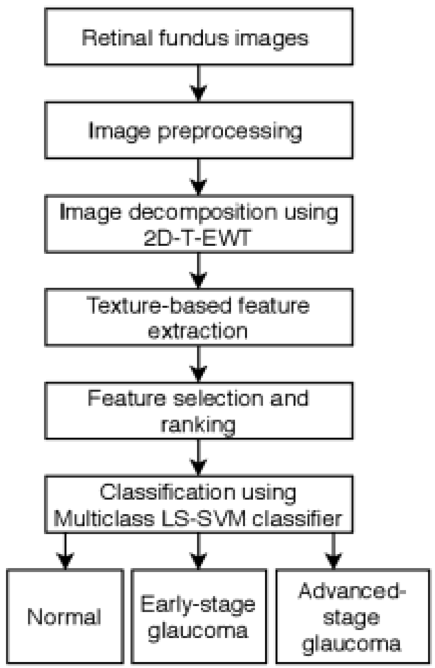

Fig.3.Thebockdiagramoftheproposedframework.

on stopping criteriaand interpolation techniques. To avoid the limitations of dyadic DWT and EMD, Gilles [18] has recently introducedanovelwavelettransformcalledempiricalwavelet transform.Afore,Gilles*etal.*[19]extendedone-dimension(1D) EWT to 2D EWT for image analysis. The EWT has various desirablepropertieslike;itisanadaptiveandsignal-dependent algorithm.Themainideaistobuildawaveletfilterbankusing Fourier supports. The advantages of the EWT as compared to the EMD is that we can adaptively use the classic wavelet for representation andEWTgives amoreconsistentdecomposition ascomparetoEMD.ThesepropertiesofEWTinspiredustouse 2DEWTbasedalgorithmintheproposedmethodforglaucoma classification.Itcanbeobservedfromtheliteraturethatnoneof the methods can be applied over a public database. The block diagram of the proposed framework is shown in Fig. 3.

Themaincontributionsofthisletterareasfollows.(1)Anovel methodis proposedfor theclassificationofglaucomastages usinganewlyintroduced2D-T-EWTimagedecomposition algorithm. (2) The main idea of the EWT based algorithm isto build a wavelet filter bank using Fourier supports. (3) The proposedmethodachievehigherclassificationaccuracythan the existing approaches. (4) The performance of the proposed methodisappliedtothepublicdatabaseforafaircomparison. The remainder of the letter is as follows. The database and theproposedmethodisexplainedindetailinSectionII.In SectionIII,wehavediscussedtheexperimentalresults.The conclusionofthepaperisprovidedinSectionIV.Thereferences are given in Section V.

II. PROPOSEDMETHOD

A. Database

In this study, we use 505 fundus images (255 normal and 250 glaucomatous images) from RIM-ONE [14] database for the binary classification. These images are stored in the 24-bit JPEGfileformatandresizedwiththeresolutionof240×240 pixelsusingbi-cubicinterpolationtoreducethecomputational complexity.RIM-ONEdatabaseispubliclyonlineavailableat http://medimrg.webs.ull.es/. Furthermore, we collect 867 fundus images (289 normal, 289 early-stage glaucoma, and 289 advanced-stage glaucoma) from Harvard Dataverse, V1 [15] databaseforthethree-classclassification.Thesefundusimages areobtainedfromKim'seyehospital.Theseimagesaretakenusinganonmydriaticautomaticfunduscamera(AFC-330Nidek). These images were cropped at the optic nerve region with the sizeof240×240 pixels forthesameresolution.These public databases serve as benchmarking data for automatic glaucoma detection.

B. Image Decomposition using 2D-Tensor-Empirical Wavelet Transform

In this work, image preprocessing is used to improve image quality [6]–[9]. It is applied to remove inappropriate variations presents in the image like noise, varying light intensity, and low contrast [2], [3]. Then, green channel images have improved using contrast limited adaptive histogram equalization. It increases a dynamic range and contrast of the input image [3], [8]. Furthermore, 2D-T-EWT is applied for image decomposition [19]. EWT is a signal-dependent approach. It cannotusepredefinedbasisfunctionslikeinFouriertransform [17]–[19].Thebasicideaistobuildawavelettightframe,which is equivalent to an adaptive filter bank [18]. The main steps include in EWT are as follows; it detects the Fourier supports and built the corresponding wavelet and filter the input signal with the obtained filter bank to get the various SBIs [7], [17]. We use the classic wavelet transform to define EWT in which thedetailcoefficientsarecorrespondingtoempiricalwavelets. Theapproximationcoefficientsarecorrespondingtothescaling function [19]–[21].

Previously,EWTbasedmethodisusedindifferentbiomedical applications[7],[17],[20],and[21].TheEWTbasedalgorithm reliesonthefrequencyspectrumofthesignal.Inthe2D-EWT basedapproach,weuseatensorproductasforclassicwavelets, whichmeansexecutetherowsandthenthecolumnsoftheinput image with the 1D-EWT algorithm [19]. First, we consider a meanspectrumfortherows(orthecolumns),thenexecutethe detectionoftheFouriersupportsusingthismeanrowspectrum. Then, we used the same filters for all rows (or columns) [18]. The2D-T-EWTmethodperformsthegivensteps[7],[19].(We denotes the $a$input image, $N_R$is thenumber of filters foreach row, and $N_C$is the number of filters for each column).

1) Performthe1DFFTofeachrow$i$of$a$;$\hat{a}(i,\omega)$;and calculatethemeanspectrummagnitudeforrows:

$$\tilde{A}_{row} = \frac{1}{N_{row}} \sum_{i=0}^{N_{row}} \hat{a}(i,\omega) \tag{1}$$

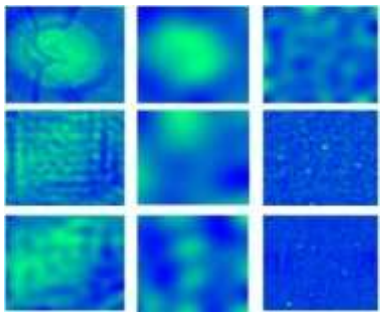

Fig.4.2D-T-EWTdecomposedcomponentsofFig.2(c),(ForN_R= 3, N_C= 3)

2) Performthe1DFFTofeachcolumn$j$of$a$;$\hat{a}(\omega,j)$;and calculate the mean spectrum magnitude for the column:

$$\tilde{A}_{column} = \frac{1}{N_{column}} \sum_{i=0}^{N_{column}} \hat{a}(\omega,j) \quad (2)$$

3) Executetheboundariesdetectionon$\tilde{A}_{row}$andbuildthe correspondentfilterbank$\{o_1^{row},\{\psi_n^{row}\}_{n=1}^{N_R}\}$,

4) Executetheboundariesdetectionon$\tilde{A}_{column}$andbuild thecorrespondentfilterbank$\{o_1^{column},\{\psi_n^{column}\}_{n=1}^{N_C}\}$,

5) Filter$a$alongtherowswith$\{o_1^{row},\{\psi_n^{row}\}_{n=1}^{N_R}\}$which provides$N_R+1$outputimages,

6) Filtereachearlierresultantimagealongwiththecolumns with$\{o_1^{column},\{\psi_n^{column}\}_{n=1}^{N_C}\}$,thisgivesattheend $(N_R+1)(N_C+1)$sub-bandimages.

In this study, the preprocessed images are decomposed into different SBIs using 2D-T-EWT. The EWT decomposed sub-bandimagesofFig.2(c)areshowninFig.4,foradvanced-stage glaucoma image.

C. FeatureExtraction

In this study, texture-based features are extracted from the 2D-T-EWTdecomposedcomponents[6],[7].Texturefeaturesare useful to measures smoothness, pixel regularities, and coarse-ness [2], [6]. The statistical approaches are employed for analysis of the spatial distribution of grey values from local features extraction.Weusesecond-ordergraylevelco-occurrencematrix (GLCM) [2], [9]. Four most significant GLCM features are energy,contrast,correlation,andhomogeneity[6],[9].Thechip histogram features are statistical texture feature, in which six features are extracted, mean, variance skewness, entropy [3], [8], energy, and kurtosis. We also used seven significant moment invariance features [2], [6].

D. FeatureNormalization,Selection,andRanking

Feature normalization improves the overall performance of the machine-learning model [10], [11]. In this study, the ex-tractedfeaturesarenormalizedusingthez-scorenormalization algorithm [3], [6]–[9]. Further, the selection of robust features ishelpingtoenhancetheclassificationperformanceintermsof accuracy [3], [6].

Inthisstudy,weusethestudent'st-testalgorithmforfeature selection and ranking of the features based on the t-value [7]. We have considered features with higher t-value first because features with high t-value are more discrimination ability [7], [10].Inthiswork,twelverobustfeaturesareselectedfrom

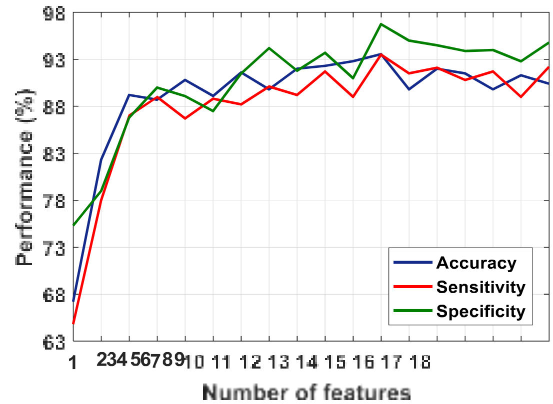

Fig.5.Agraphbetweenofperformancemeasuresandthenumberoffeaturesfor three-class classification

TABLE I

CONFUSIONMATRIXFORBINARYCLASSIFICATION

	Normal	Glaucoma
Normal	234	21
Glaucoma	17	233

twenty-ninefeatures,whichareextractedfromthreedifferent texturefeatureset.

E.ClassificationusingKernel-BasedMulticlass LS-SVM Classifier

Inthisstudy,MC-LS-SVMclassifierhasbeenusedforglau-coma classification. The support vector machines are a set of supervised learning algorithms, widely used as a classifier to classify two or more classes [3], [22]. In SVM, hyper-planes are employed to create a decision boundary for the classifi-cation using radial basis function (RBF) kernel [3], [6]–[10].It can be seen from the literature that one-against-one method ismoresuitablethantheone-against-allmethodformulticlass classification.Toimplementtheone-against-onealgorithmfor the classifier, we consider the number of classes(n class) ,andthenn class×(n class−1)/2 classifiersareusedforeach one-trained data from two stages [3], [13]. The MC-LS-SVM classifier is used in various biomedical applications such as classificationofglaucomastages[13],andclassificationofsleep stages based EEG signals [24].

III. RESULTSANDDISCUSSION

In this study, 2D-T-EWT [19] image decomposition algorithm has been used for performance enhancement, because EWT [17],[18]showssignificantadvantagesoverconventionalmeth- ods DWT [2] and EMD [16]. In this work, the pre-processed images are decomposed into various SBIs using 2D-T-EWT [19]. Then, various texture-based features have been extracted from the decomposed components. The variation in the clas-sification accuracy with the number of features is shown in Fig. 5. This plot shows that only twelve robust features are qualified to achieve the highest accuracy. In Fig. 6, the RBF kernel parameter(σ) is varied from 0.3 to 3 with an increment of 0.3, the classification performance can be enhanced withthe suitable selection of σ [3], [7]. The obtained confusion matrixesoftheclassifieraftertenfoldcross-validationforbinary andthree-stageclassificationisprovidedinTablesIandII,

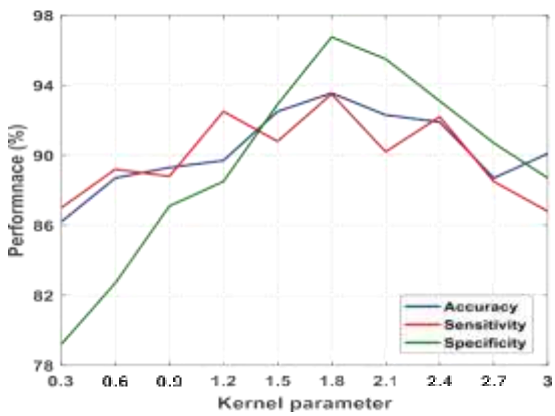

Fig.6.AgraphbetweenperformanceparametersandRBFkernelparameterafter tenfold cross-validation.

TABLE II
CONFUSIONMATRIXFORTHREE-CLASSCLASSIFICATION

	Normal	Early-stage	Advanced-stage
Normal	275	6	8
Early-stage	13	264	12
Advanced-stage	8	8	273

TABLEIII
CLASSIFICATIONRESULTSOFTHEPROPOSEDMETHODON DIFFERENTDATASETS

Database	Ac (%)	Sn (%)	Sp (%)	F2 (%)	AUC
Drishti-GS [26]	85.20	84.67	87.10	85.50	0.8589
HRF [28]	86.34	88.10	84.34	86.70	0.8622
LES-AV [29]	90.30	92.50	89.67	90.87	0.9108
RIM-ONE [14]	92.47	93.20	91.67	92.90	0.9243

respectively. In this study, five indicators are used for performance measurement namely, accuracy (Ac), sensitivity/recall (Sn),specificity(Sp)[6],[30],receiver-operatingcharacteristic (ROC)intermsofareaundertheROC(AUC),andF-score(F2) ($F_\beta=(1+\beta^2)\times Pr\cdot Sn/(\beta^2\cdot Pr)+Sn$;wherePr:presci- sion, set β = 2).

More recently, many approaches have been proposed for binaryclassificationusingRIM-ONEdatabase.Inrelatedstud- ies [6], [7], and [9] achieves accuracies of 83.60%, 80.66%, and 86.13%, respectively. Lately, the method [3] obtained an accuracy of 90.76%. Whereas, our method achieved the highest accuracy of 92.47% on RIM-ONE data-base. Besides, the effectiveness of the proposed method has been evaluated on differentdatasets(Drishti-GS,HRF,LES-AV,andRIM-ONE); the obtained results are shown in Table III. It can be seenfromTableIII,thattheproposedmethodachievesbetterresults on RIM-ONE database. The obtained results in terms of Ac, Sn,Sp,F2,andAUCas92.47%,93.20%,91.67%,92.90%, and 0.9243, respectively. The performance comparison of the state-of-the-artapproachesonRIM-ONEdatabaseisshownin TableIV.Besides,theproposedmethodhasbeencomparedwith advanced deep learning methods (NightOwl and WinterFell) [25].Forafaircomparison,weusedthreeindicatorsSn,Sp,and AUC.ItcanbeseenfromTableVI,thatourmethodachieved betterperformancethan[25],asitachievedthehighestAUCof 0.9503.

Forthethree-classclassification,Noronha*etal.*[13]reported 90.07%accuracyusingSVMclassifierontheprivatedatabase.

TABLE IV
PERFORMANCECOMPARISONWITHTHESTATE-OF-THE-ARTAPPROACHESONTHE RIM-ONE DATABASE [14]

Database	Method	Ac (%)	Sn (%)	Sp (%)	F2 (%)	AUC
RIM-ONE.	Maheshwari et al. [7]	80.66	78.00	88.23	80.90	0.8140
	Kirar et al. [6]	83.60	86.4	80.80	85.58	0.8357
	Agrawal et al. [9]	86.13	84.8	87.43	86.70	0.8710
	Parashar et al. [3]	90.76	94.5	87.84	90	0.9117
	Ours	**92.47**	93.20	91.67	92.90	0.9243

TABLE V
PERFORMANCEOFTWODIFFERENTMETHODSFORTHREE-CLASS CLASSIFICATION ONTHE SAME DATABASE [15]

Database	Method	Ac (%)	Sn (%)	Sp (%)	F2 (%)	AUC
HARVARD DATAVERSE, V1	Noronha et al. [13]	88.34	87.75	91.50	88.80	0.8965
	Ours	**93.65**	93.50	96.67	94.07	0.9510

TABLE VI
PERFORMANCECOMPARISONOFTHEPROPOSEDMETHODWITHADVANCED DEEPLEARNINGMETHODSONREFUGETESTSET[25]

Training set	Method	Sn (%)	Sp (%)	AUC
REFUGE [25]	NightOwl [25]	90	85	0.9101
	Ours	94.30	89.90	**0.9210**
ORIGA [27]	WinterFell [25]	92.50	85	0.9327
	Ours	96.40	93.67	**0.9503**

This private database is not available as benchmarking data to evaluateimage-processingalgorithmsforglaucomaclassifica- tion. For a fair comparison, the conventional method [13] has been evaluated on the Harvard Dataverse, V1 public database. Theobtainedresultsfor[13]intermsofAc,Sn,Sp,F2,andAUC as88.34%,87.75%,91.50%,88.80%,and0.8965respectively. Whereasonthesamedatabase,ourmethodachievedfarbetter resultsintermsofAc,Sn,Sp,F2,andAUCas93.65%,93.50%, 96.67%, 94.07%, and 0.9510, respectively. The performance comparison of the proposed method with the conventional method [13] on Harvard Dataverse, V1 database is providedin Table V In summary, the proposed method outperformed state-of-the-art approaches for glaucoma classification.

IV. CONCLUSION

We employed the recently released 2D-T-EWT based algorithm for image decomposition in this letter. It was discovered that the deconstructed components of 2D-T-WET are valuable for texture-based feature extraction.The student test algorithm is used to pick and rank these retrieved attributes.Using the MC-LS-SVM classifier, we have found that only twelve robust characteristics are qualified to attain the greatest classification accuracy. As a result, compared to the current methods, the suggested method has reduced computing complexity and more accuracy. Tenfold cross-validation has been used to assess the efficacy of the suggested approach.The findings collected demonstrate that our strategy for classifying glaucoma performed better than state-of-the-art approaches. Because the suggested method has an accuracy of 91.34% in detecting glaucoma in its early stages, it can be employed effectively and reliably for glaucoma diagnosis.In subsequent work, we want to use deep learning models to increase classification performance.

REFERENCES

[1] W. M. Liao, B. Zou, R. C. Zhao, Y. Q. Chen, Z. Y. He, and M. J. Zhou,"Clinicalinterpretabledeeplearningmodelforglaucomadiagnosis," *IEEE J.Biomed.HealthInform.*,vol.24,no.5,pp.1405–1412,2020.

[2] B.S.Kirar,D.K.Agrawal,andS.Kirar,"Glaucomadetectionusingimagechannelsanddiscrete wavelettransform," *IETEJ.Res.*, tobepublished,doi:10.1080/03772063.2020.1795934.

[3] D. Parashar and D. K. Agrawal, "Automated classification of glaucoma stages using flexible analytic wavelet transform from retinalfundus images," *IEEE Sensors J.*, vol. 20, no. 21, pp.12885–12894,Nov.2020.

[4] A. T. Nguyen, D. S. Greenfield, A. S. Bhakta, J. Lee, and W. J. Feuer,"Detectingglaucomaprogressionusingguidedprogressionanalysis withOCTandvisualfieldassessmentineyesclassifiedbyinternationalclassificationofdiseaseseveritycodes,"*Amer.Acad.Ophthalmol.,Ophthalmol.Glaucoma*, vol. 2, no. 1, pp. 36–46, 2019.

[5] T.C.Lim,S.Chattopadhyay,andU.R.Acharya,"Asurveyandcomparativestudyontheinstrumentsforglaucomadetection,"*Med.Eng.Phys.*,vol. 34, pp. 129–139, 2012.

[6] B. S. Kirar and D. K. Agrawal, "Computer aided diagnosis of glaucomausingdiscreteandempiricalwavelettransformfromfundusimages,"*IETImage Process.*, vol. 13, no. 1, pp. 73–82, 2019.

[7] S.Maheshwari,R.B.Pachori,andU.R.Acharya,"Automateddiagnosisofglaucomausingempiricalwavelettransformandcorrentropyfeaturesextracted fromfundusimages,"*IEEEJ.Biomed.HealthInform.*,vol.21,no. 3, pp. 803–813, 2017.

[8] S.Maheshwari,V.Kanhangad,R.B.Pachori,S.V.Bhandary,and U.R.Acharya,"Iterativevariationalmodedecompositionbasedautomateddetection ofglaucomausingfundusimages,"*Comput. Biol.Med.*,vol.88, pp.142–149,May2017.

[9] D. K. Agrawal, B. S. Kirar, and R. B. Pachori, "Automated glaucomadetectionusingquasi-bivariatemodedecompositionfromfundusimages,"*IET Image Process.*, vol. 13, no. 13, pp. 2401–2408, 2019.

[10] U. R. Acharya, S. Dau, X. Du, and S. V. Sree, "Automated diagnosis ofglaucoma using texture and higher order spectra features," *IEEE Trans.Inf. Technol. Biomed.*, vol. 15, no. 3, pp. 449–455, May 2011.

[11] U.R.Acharya*etal.*,"Automatedscreeningsystemforretinalhealthus-ingbi-dimensionalempiricalmodedecompositionandintegratedindex,"*Comput. Biol. Med.*, vol. 75, no. 1, pp. 54–62, 2016.

[12] L.Li*etal.*,"Alarge-scaledatabaseandaCNNmodelforattention-basedglaucomadetection,"*IEEETrans.Med.Imag.*,vol.39,no.2,pp.413–424,Feb.2020.

[13] K. P. Noronha, U. R. Acharya, K. P. Nayak, R. J. Martis, and S. V.Bhandary, "Automated classification of glaucoma stages using higherordercumulantfeatures,"*Biomed.SignalProcess.Control*,vol.10, pp.174–183,2014.

[14] F.Fumero,S.Alayon,J.L.Sanchez,J.Sigut,andM.Gonzalez-Hernandez,"RIM-ONE:Anopenretinalimagedatabaseforopticnerveevaluation,"in*Proc.24thIEEEInt.Symp.Comput.-BasedMed.Syst.*,2011,pp.1–6.

[15] J.M.Ahn, S.Kim, K.-S.Ahn, S.-H.Cho, K.B. Lee,andU. S.Kim, "A deeplearningmodelforthedetectionofbothadvancedandearlyglaucomausing fundus photography," *PLoS ONE*, vol. 13, no. 11, pp.1–8, 2018,Art. no. e0207982.

[16] N. E. Huang *et al.*, "The empirical mode decomposition and the hilbertspectrumfornonlinearandnon-stationarytimeseriesanalysis,"*Proc.Roy.Soc. A: Math., Phys. Eng. Sci.*, vol. 454, pp. 903–995, 1998.

[17] A.BhattacharyyaandR.B.Pachori,"Amultivariateapproachforpatientspecificeegseizuredetectionusingempiricalwavelettransform,"*IEEETrans. Biomed. Eng.*, vol. 64, no. 9, pp. 2003–2015, Sep. 2017.

[18] J. Gilles, "Empirical wavelet transform," *IEEE Trans. Signal Process.*,vol. 61, no. 16, pp. 3999–4010, Aug. 2013.

[19] J. Gilles, G. Tran, and S. Osher, "2D empirical transforms: Wavelets,ridgelets,andcurveletsrevisited,"*SIAMJ.Imag.Sci.*,vol.7,no.1, pp.157–186,2014.

[20] A. Bhattacharyya, L. Singh, and R. B. Pachori, "Fourier–Bessel seriesexpansionbasedempiricalwavelettransformforanalysisofnon-stationarysignals," *Digit. Signal Process.*, vol. 78, pp. 185–196, 2018.

[21] A. Anuragi, D. Sisodia, and R. B. Pachori, "Automated alcoholism detection using Fourier–Bessel series expansion based empirical wavelettransform," *IEEE Sensors J.*, vol. 20, no. 9, pp. 4914–4924, 2020.

[22] J.A.K.SuykensandJ.Vandewalle,"Leastsquaressupportvectormachineclassifiers," *Neural Process. Lett.*, vol. 9 no. 3, pp. 293–300, 1999.

[23] S.TaranandV.Bajaj,"SleepapneadetectionusingartificialbeecolonyoptimizehermitebasisfunctionsforEEGsignals,"*IEEETrans.Instrum.Meas.*, vol. 69, no. 2, pp. 608–616, Feb. 2020.

[24] V.BajajandR.B.Pachori,"Automaticclassificationofsleepstagesbasedonthetime-frequencyimageofEEGsignals,"*Comput.MethodsProgramsBiomed.*, vol. 112, no. 3, pp. 320–328, 2013.

[25] J. I. Orlando *et al.*, "REFUGE challenge: A unified framework forevaluating automated methods for glaucoma assessment from fundusphotographs," *Med. Image Anal.*, vol. 59, Jan. 2020, Art. no. 101570,doi:10.1016/j.media.2019.101570.

[26] J.Sivaswamy,S.R.Krishnadas,G.D.Joshi,M.Jain,andA.U.S.Tabish,"Drishti-GS:Retinalimagedatasetforopticnervehead(ONH)segmen-tation," in *Proc. IEEE 11th Int. Symp. Biomed. Imag.*, Apr./May 2014, pp.53–56.

[27] Z. Zhang *et al.*, "ORIGA-light: An online retinal fundus image databaseforglaucomaanalysisandresearch,"in*Proc.Annu.Int.Conf.IEEEEng.Med. Biol.*, Aug./Sep. 2010, pp. 3065–3068.

[28] J. Odstrcilik *et al.*, "Retinal vessel segmentation by improved matchedfiltering: Evaluation on a new high-resolution fundus image database,"*IET Image Process.*, vol. 7, no. 4, pp. 373–383, Jun. 2013.

[29] J. I. Orlando *et al.*, "Towards a glaucoma risk index based on simulatedhemodynamicsfromfundusimages,"in*Proc.int.Conf.Med.ImageCom-put.Comput.Assist.Interv.*,Granada,Spain,vol.11071,2018,pp.65–73.

[30] J. I. Orlando, E. Prokofyeva, and M. B. Blaschko, "A discriminativelytrained fully connected conditional random field model for blood vesselsegmentationinfundusimages,"*IEEETrans.Biomed.Eng.*,vol.64,no.1, pp.16–27,Jan. 2017.